Talanta 91 (2012) 110–115

Contents lists available at SciVerse ScienceDirect

Talanta

journal homepage: www.elsevier.com/locate/talanta

Carbon nanotubes-ionic liquid nanocomposites sensing platform for NADH oxidation and oxygen, glucose detection in blood

Lu Bai[a], Dan Wen[a], Jianyuan Yin[b], Liu Deng[a], Chengzhou Zhu[a], Shaojun Dong[a,*]

[a] State Key Laboratory of Electroanalytical Chemistry, Changchun Institute of Applied Chemistry, Chinese Academy of Sciences, Changchun, Jilin 130022, PR China
[b] Department of Traditional Chinese Medicinal Chemistry, Pharmacy College, Jilin University, Changchun 130021, PR China

ARTICLE INFO

Article history:
Received 20 October 2011
Received in revised form 11 January 2012
Accepted 12 January 2012
Available online 18 January 2012

Keywords:
Carbon nanotubes
Ionic liquid
Electrochemical sensing
Blood samples

ABSTRACT

An excellent electrochemical sensing platform has been designed by combining the huge specific surface area of carbon nanotubes (CNTs) and the remarkable conductivity of ionic liquid (IL). IL can easily untangle CNTs bundles and disperse CNTs by itself under grinding condition due to the π–π interaction between CNTs and IL. The resulting nanocomposites showed an augmentation on the voltammetric and amperometric behaviors of electrocatalytic activity toward O_2 and NADH. Therefore, such an efficient platform was developed to fabricate mediator-free oxygen sensor and glucose biosensor based on glucose dehydrogenase (GDH). O_2 could be determined in the range of zero to one hundred percent of O_2 content with the detection limit of 126 μg L^{-1} (S/N = 3). The glucose biosensor which was constructed by entrapping GDH into chitosan on the nanocomposites modified glassy carbon electrode surface, exhibited good electrocatalytic oxidation toward glucose with a detection limit of 9 μM in the linear range of 0.02–1 mM. We also applied the as-prepared sensors to detect oxygen and glucose in real blood samples and acquired satisfied results.

1. Introduction

Due to their significant electric, thermal and mechanical properties, carbon nanotubes (CNTs) have obtained great attention in a variety of fields, such as electrochemical sensors, tissue engineering, and energy storage devices [1–5]. In particular, the ability of CNTs modified electrodes to promote electron-transfer reactions and resist to surface fouling make them extremely attractive for fabricating electrochemical sensors [6–8]. The unique properties of CNTs can be readily tuned by controllable functionalization using covalent and noncovalent procedures, for example, different recognition molecules including glucose, neurotransmitters and cancer biomarkers have been conjugated to functionalized CNTs for analytical applications [9–13]. Though covalently functionalized CNTs can be reliably obtained by chemical treatment [14,15], some of the important properties are lost due to partial destruction of their conjugated π system. To preserve the sp^2 nanotube structure, noncovalent modification of CNTs via π–π interactions is essential.

Ionic liquid (IL) is a kind of important solvent with unique properties of good ionic conductivity, high viscosity, negligible vapor pressure, high chemical and thermal stabilities, and low toxicity. Hence, it has been widely applied in electrochemistry [16–18]. Owing to the non-covalent (π–π) interactions between the loop of imidazole IL and the π electronic of CNTs, IL can easily untangle CNT bundles and disperse CNTs by itself under grinding condition without destroying the symmetry structure and conjugated π system of CNTs [19]. As a result, the combination of IL and CNTs could provide a striking synergistic augmentation performance like good electronic and ionic conductivity, high electrochemical stability, and good biocompatibility. This strategy is also wildly investigated in electrochemical fields such as biosensors, electric double-layer capacitors, electrochemical actuators, and biofuel cells [20–23]. Our group has found that the carbon nanotubes-ionic liquid (CNTs-IL) gel modified electrode had excellent electrochemical properties and good biocompatibility, where the immobilized laccase and glucose oxidase exhibited good stability and enhanced electrocatalytic ability [24,25]. Chitosan (CS), CNTs and IL biocompatible components were used to fabricate a composite ionic actuator and the good compatible of IL with CNTs and CS allows their effective transportation between electrodes, exhibiting remarkable bending actuation performance at low applied voltage [21]. Interestingly, based on the special characteristics of polymeric IL which provides the possibility of π-stacking interactions with the aromatic sidewalls of the nanotubes, water and organic stable dispersions of CNTs can be reversibly switched by simply exchanging the counter anion of the attached polymeric IL [26]. These demonstrations show that the use of IL paves an efficient way to the functionalization of CNTs.

Both oxygen and glucose are involved in the essential cellular functions, for example, they are consumed in energy production

* Corresponding author. Tel.: +86 431 85262101; fax: +86 431 85689711.
E-mail address: dongsj@ciac.jl.cn (S. Dong).

0039-9140/$ – see front matter © 2012 Elsevier B.V. All rights reserved.
doi:10.1016/j.talanta.2012.01.027

where oxygen as an electron acceptor and glucose as an electron donor [27]. Some pathological events may be caused when their content is abnormal, so it is of importance to reliable and fast monitor oxygen and glucose concentration for the treatment and control of disease. Additionally, NADH is a vital cofactor in over 300 dehydrogenase-based enzymatic reactions [28]. Oxidation of NADH at electrodes surfaces has attracted great interest due to its significant both a cofactor for dehydrogenase and its role in the biological electron transfer chain systems [29]. In the present work, CNTs-IL nanocomposites were formed by simply grinding. It is found that the composites showed excellent electrocatalytic activities toward O_2 and NADH and consequently we exploited their potential applications as oxygen and glucose sensing. On one hand, CNTs-IL nanocomposites were used to directly detect O_2, on the other hand, glucose dehydrogenase (GDH) was immobilized on the CNTs-IL nanocomposites surface to fabricate a glucose biosensor. To further exploit their potential practical application, we applied these sensors to detect oxygen and glucose in real blood samples.

2. Experimental

2.1. Reagents

Multiwalled carbon nanotubes purchased from Shenzhen Nanotech. Port. Co. Ltd. (Shenzhen, China) were used without further purification. 1-Butyl-3-methylimidazolium hexafluorophosphate ($BMIMPF_6$) IL purchased from J&K Chemical Ltd. was used without pretreatment. GDH (E.C. 1.1.1.47, thermoplasma acidophilum, recombinant expressed in *Escherichia coli*) and CS were obtained from Sigma Chemical Co. NADH, NAD^+ and β-D-(+)-glucose were purchased from Beijing Chemical Reagent. Glucose stock solution was kept for 24 h before use. All other chemicals were of analytical grade and the solutions were prepared with the doubly distilled water.

2.2. Preparation of modified electrodes

CNTs-IL nanocomposites were prepared by hand-mixing CNTs and IL ($BMIMPF_6$). Briefly, 2 mg CNTs and 20 μL IL were mixed in an agate mortar and then ground for about 15 min to form a viscous gel. Glassy carbon electrode (GCE, 3 mm in diameter) was polished with 1.0 and 0.3 μm alumina slurry sequentially and then washed ultrasonically in water and ethanol for a few minutes, respectively. A small quantity of the CNTs-IL gel was immobilized on the GCE surface and smoothed on a weighing paper to get an even film covering the electrode surface (noted as CNTs-IL/GCE). GDH was entrapped into CS to develop a glucose biosensor. CS was dissolved in 1% acetic acid solution. After CNT-IL/GCE was prepared, 8 μL GDH (1 mg L^{-1}) and CS mixture (v:v = 2:1) was dropped on the CNTs-IL/GCE surface and dried at 4 °C for 12 h. It was noted as GDH-CS/CNTs-IL/GCE.

2.3. Instruments

The morphology of CNTs-IL nanocomposites were obtained by scanning electron microscopy (SEM, PHILIPS XL-30), operated at an accelerating voltage of 20.0 KV. Electrochemical impedance spectroscopy (EIS) was performed with an Autolab/PGSTAT 30 (Eco Chemie B.V. Utrecht, The Netherlands) in a grounded Faraday cage. In the presence of 5.0 mM $Fe(CN)_6^{3-/4-}$ and 0.02 M KCl, the EIS measurements were carried out at a basis potential of 0.24 V under an oscillation potential of 5 mV over the frequency range of 1 Hz to 100 kHz. All other electrochemical measurements were performed with a CHI 832 C electrochemical workstation (Chenhua Co., Shanghai) and carried out in a conventional three-electrode system. The modified GCEs were used as the working electrode. Platinum foil and Ag/AgCl (saturated KCl) were used as the counter electrode and the reference electrode, respectively. An EG & PARC model 636 rotating ring-disk electrode system was used for rotating disk electrode (RDE) experiments. A rotating glassy carbon disk platinum ring electrode was used as the working electrode. YSI-58 dissolved oxygen meter was used to detect dissolved oxygen as a standard. Calibrations are needed before use.

2.4. Measurements

Chronoamperometry was used to measure the concentration of O_2 on CNTs-IL/GCE with applied potential of −0.2 V. For the extending liner range of O_2 experiment, N_2, air and O_2 saturated solutions were set as 0, 20.95% and 100% of O_2 content, respectively. The calibration curve for glucose on GDH-CS/CNTs-IL/GCE was obtained by the peak current of cyclic voltammetry.

For the real detection, human blood samples were obtained from local hospital and centrifuged to separate erythrocytes and the serum. The supernatant solution was collected to detect blood glucose without any purification. Then the left erythrocytes were wash 3 times with a cold isotonic PBS buffer (0.145 M NaCl, 1.9 mM NaH_2PO_4, 8.1 mM Na_2HPO_4, pH 7.4) and suspended in PBS for oxygen detection. Before measurements, the sample was saturated with N_2.

3. Results and discussion

3.1. Characterization of CNTs-IL nanocomposites

We first characterized morphology of the formed CNTs-IL nanocomposites with SEM. Fig. 1A showed the typical SEM image of the CNTs-IL nanocomposites spread on GCE. It was observed that the substrate was covered with a great deal of tube-shape nanostructures. IL untangled CNTs to form a gel with uniform surface. Here, the cation–π and/or π–π interaction between CNTs and IL played an important role in the formation of the homogeneous nanotubes structure [19]. Without further purification, CNTs were well dispread in IL and the nanostructure retained at least one month in air, so the resulting nanocomposites were highly stable. Moreover, after 1000 cycles voltammetric potential cycling (100 mV s^{-1}) of CNTs-IL/GCE, the current still retained 96.9% of its initial value, demonstrating good stability of the modified electrode.

The electrochemical properties of CNTs-IL nanocomposites were further exploited by electrochemical impedance measurements and cyclic voltammetry. EIS is a useful method to probe the electrical properties of interface between modified electrodes and electrolyte. $Fe(CN)_6^{3-/4-}$ was used as the electrochemical probe to distinguish impedance characters of the CNTs and CNTs-IL nanocomposite. The electron transfer resistance (R_{ct}) can be estimated by the semicircle diameter of the impedance spectra at high frequency range. On the bare GCE, the R_{ct} was estimated to be 474 Ω (black line in Fig. 1B). After the CNTs modification of GCE surface, the R_{ct} decreased sharply to 14 Ω (red line in Fig. 1B). The R_{ct} decrease of modified electrode could be attributed to the excellent electronic conductivity of CNTs, and the electron transfer was effective. When CNTs-IL nanocomposites were modified on GCE surface, the impedance spectroscopy curve was almost a straight line at higher frequencies as shown in Fig. 1B, indicating that the combination of IL and CNTs could provide a considerable electrochemical augmentation performance.

The cyclic voltammograms (CVs) of the CNTs-IL nanocomposites modified electrode at different scan rates were displayed in Fig. 1C. The anodic and cathodic peak currents were directly proportional to the scan rates from 10 to 100 mV s^{-1}, demonstrating a surface confined redox process (Fig. 1D). It should be noted that the

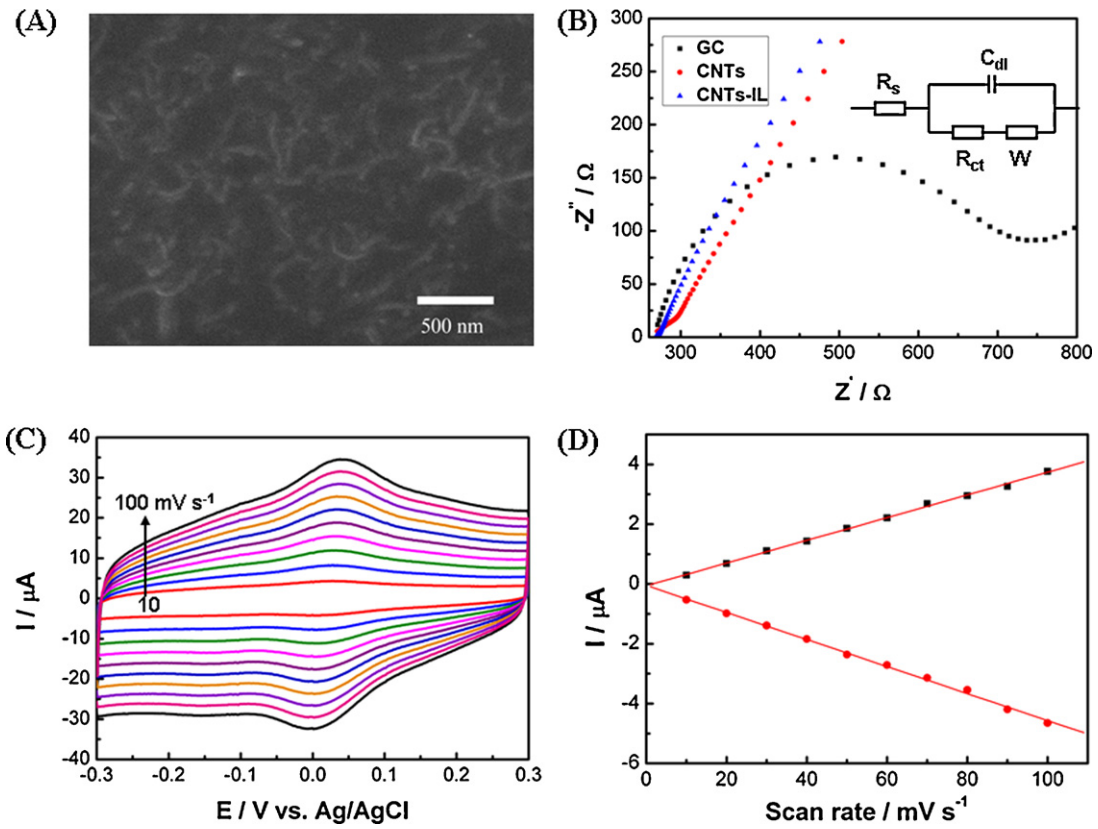

Fig. 1. (A) SEM image of CNTs-IL nanocomposites. (B) EIS of GCE (black), CNTs (red) and CNTs-IL nanocomposites (blue) modified GCEs in 0.02 M KCl solution containing 2.5 mM $K_3[Fe(CN)_6]$ and 2.5 mM $K_4[Fe(CN)_6]$. Frequency range: 10^5–1 Hz. (C) CVs of CNTs-IL/GCE in PBS (pH 7.4) with different scan rates. From inner to outer: 10, 20, 30, 40, 50, 60, 70, 80, 90 and 100 mV s^{-1}. (D) Anodic (black) and cathodic (red) peck current *vs.* scan rate. (For interpretation of the references to color in this figure legend, the reader is referred to the web version of the article.)

anodic and cathodic waves were symmetrical with small separation around 0.02 V, which showed a reversible system. The reversible peaks may be due to the electroactive groups of CNTs (*e.g.* carbonyl group) which have been reported with the similar peak potential around 0 V in the literature [30,31], and simultaneously the high conductivity of IL make them more reversible. The excellent electrochemical behaviors suggest that the CNTs-IL nanocomposites can be used as an electrochemical platform for the development of sensors and biosensors.

3.2. Electrocatalytic reduction and detection of O_2

The resulting nanocomposites of CNTs-IL exhibited good electrocatalytic activity toward reduction of O_2. Curve a in Fig. 2A showed a pair of reversible redox peaks under N_2 saturated PBS. The voltammetric features of the CNT-IL/GCE changed greatly under the presence of O_2 in solution, being characterized with a large cathodic reduction peak around −0.28 V (curve b in Fig. 2A). Compared with pure CNTs (Fig. 2B), CNTs-IL nanocomposites efficiently decreased the O_2 reduction overpotential with the onset potential of 0.08 V and enhanced the catalytic current largely.

To further investigate the electrocatalytic mechanism of the CNTs-IL nanocomposites for O_2 reduction, we carried out the linear sweep voltammetry (LSV) on a rotating disk electrode with different rotating rates (Fig. 2C). When the mass transport process in the solution and the catalytic reaction become dominant, the Levich equation reduces to the Koutecky–Levich equation [32]:

$$\frac{1}{i_l} = \frac{1}{nFAc_0k\Gamma} + \frac{1}{0.62nFAc_0D^{2/3}\nu^{-1/6}\omega^{1/2}} \qquad (1)$$

$$i_k = nFAc_0k\Gamma$$

where n, A, c_o, k, Γ, D, ν, ω represent the number of electrons transferred, the electrode area, the bulk concentration of O_2 in the solution, the reaction rate constant, the surface concentration of the catalyst, the O_2 diffusion coefficient, the kinematics viscosity, and the rotation rate, respectively. The other symbols have their usual meanings. As shown in Fig. 2D, the Koutecky–Levich plot for CNTs-IL nanocomposites is linear with a slope close to the dashed line calculated from the four-electron reduction of O_2 while the rotating disk area $A = 0.152\ cm^2$, the concentration of O_2 in air saturated buffer solution $c_0 = 2.9 \times 10^{-4}$ M, the O_2 diffusion coefficient $D = 1.7 \times 10^{-5}\ cm^2\ s^{-1}$, and the kinematic viscosity $\nu = 0.01\ cm^2\ s^{-1}$. It was found that the calculated number of electrons involved in the reduction of O_2 process was about 3.75, indicating that the reduction of O_2 at the CNTs-IL/GCE mainly supported the four-electron pathway. However, in the case of the majority carbon-based materials, the electron transfer number of oxygen reduction is close to two [33,34]. The effective O_2 reduction process of the CNTs-IL nanocomposites could be mainly attributed to reasons as follow: (1) the high catalytic active sites at CNTs; (2) through intermolecular charge transfer the positively charged nitrogen containing imidazolium loop of IL could generate positive charge on carbon atoms of CNTs plane and make O_2 absorption favorable in CNTs [2,33]; (3) the high conductivity of CNTs-IL nanocomposites; (4) heavily entangled CNTs bundles could be untangled to form much finer bundles through the cation–π and/or π–π interaction [19].

Based on the excellent electrochemical reduction activity toward O_2, CNTs-IL nanocomposites system was a promising platform to construct O_2 sensors. YSI-58 dissolved oxygen meter was used to detect O_2 as the standard. Steady-state current responses of CNTs-IL/GCE were obtained at the applied potential of −0.2 V. As shown in Fig. 3A, the CNTs-IL/GCE linearly responded to dissolved

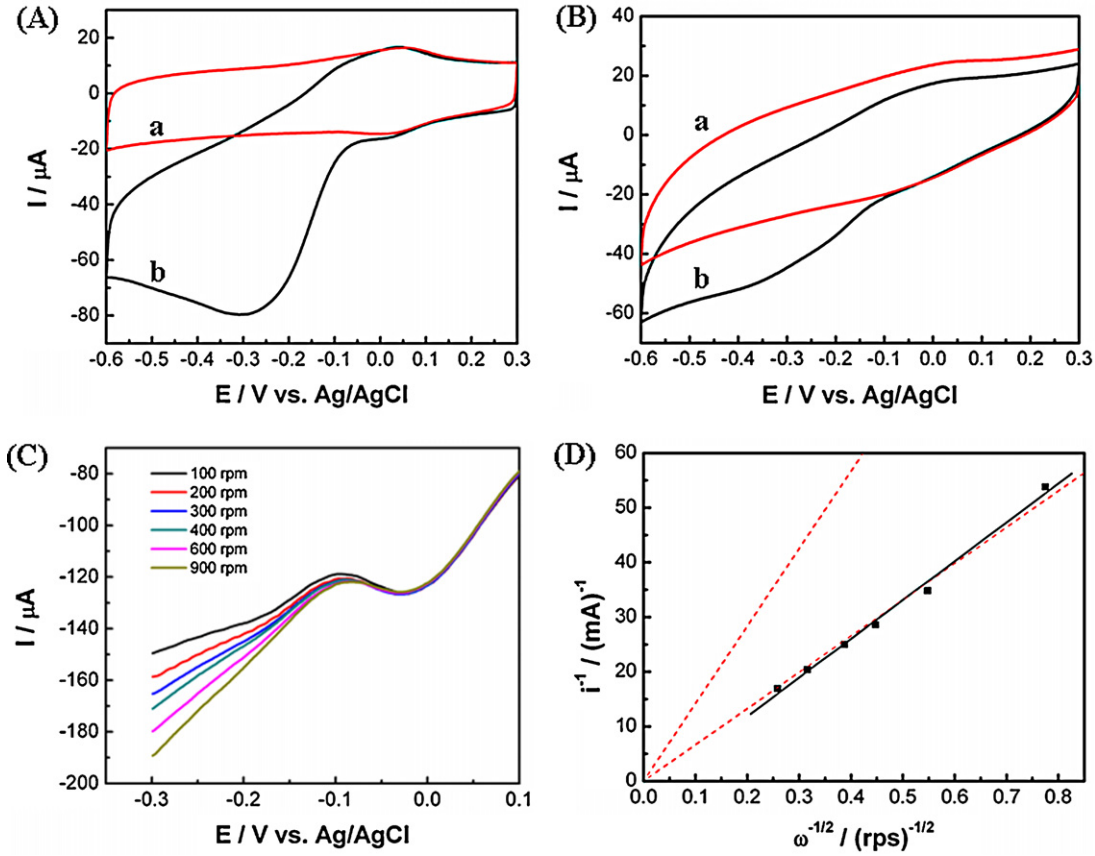

Fig. 2. CVs of (A) CNTs-IL/GCE, (B) CNT/GCE in (a) N_2 saturated and (b) O_2 saturated PBS (pH 7.4). (C) RDE voltammetry curves of oxygen reduction on CNTs-IL/GCE with different rotating rates. (D) Koutecky–Levich plots of oxygen reduction on CNTs-IL/GCE (solid line). The dashed lines are from the calculated data of two (upper) and four (down) electrons reduction of oxygen, respectively.

O_2 concentration below 20 mg L^{-1} of the dissolved oxygen meter measurement range with the detection limit of 126 μg L^{-1} (S/N = 3). Five repeats had been done and the relative standard deviation (R.S.D.) of the sensors was 5.6%. Moreover, to extend the liner range of oxygen detection, N_2, air and O_2 saturated PBS were used as the concentration standard. The calibration curve corresponding to steady-state current responses was linear against the percent of oxygen content from N_2 saturated to O_2 saturated (Fig. 3B), therefore a nanocomposites sensing for O_2 was developed in the wide range of zero to one hundred percent of oxygen content.

Since the prominent sensing performance in O_2 detection, the CNTs-IL nanocomposites based sensor was also applied to detect O_2 released from erythrocytes. $NaNO_2$ could react with heme in erythrocytes to form methemoglobin so it was used to release oxygen. No response was observed on CNTs-IL/GCE after injecting $NaNO_2$ into PBS, so the interference of $NaNO_2$ was negligible. When 2 mM $NaNO_2$ was injected into PBS containing erythrocytes, a reduction current of 0.394 μA was observed and the corresponding calculated data is 1.85 mg L^{-1} which was in good agreement with the concentration of 1.91 mg L^{-1} obtained by dissolved oxygen meter.

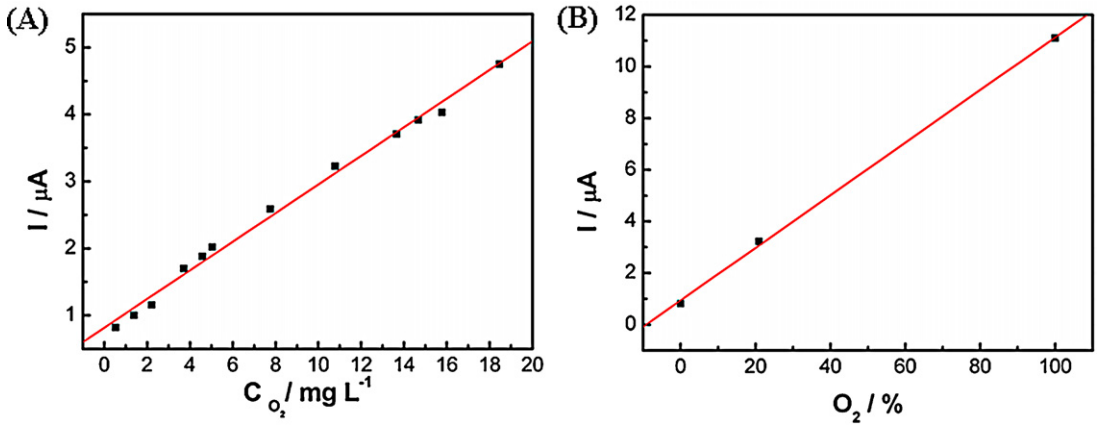

Fig. 3. (A) Calibration curve for dissolved oxygen of CNTs-IL/GCE in PBS (pH 7.4). (B) The dependence of the reduction current on percent of oxygen of CNTs-IL/GCE in PBS (pH 7.4).

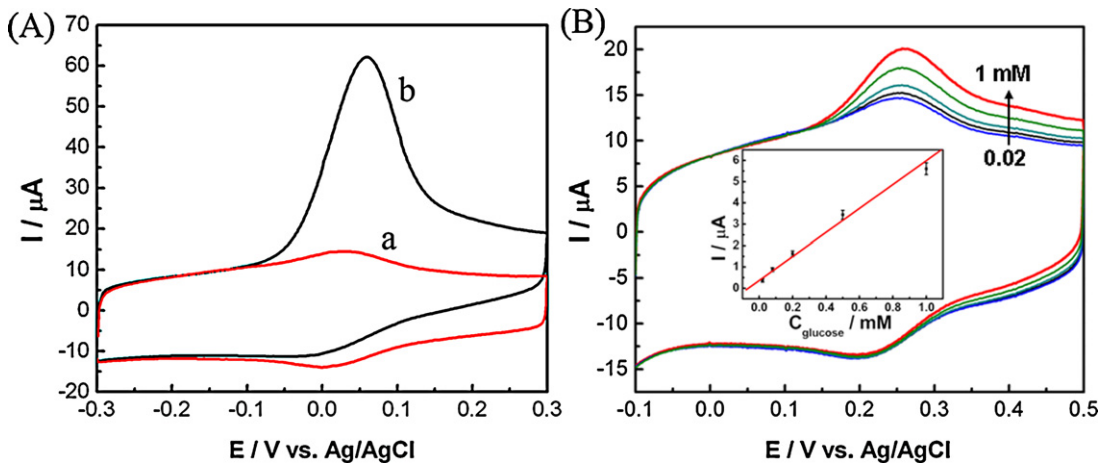

Fig. 4. (A) CVs of CNTs-IL/GCE (a) without and (b) with 1 mM NADH in PBS (pH 7.4). (B) CVs of GDH-CS/CNTs-IL/GCE in PBS (pH 7.4) with 10 mM NAD^+ containing 0.02, 0.08, 0.2, 0.5, 1 mM glucose (from inner to outer). Inset: Calibration curve for different concentration of glucose.

Therefore, CNTs-IL nanocomposites could be potentially useful for the O_2 detection in real samples.

3.3. Electrocatalytic oxidation of NADH and detection of glucose

For developing dehydrogenase-based bioelectrochemical devices, the electrocatalytic oxidation of NADH has gained great attention [35]. However, oxidation of NADH at ordinary electrode is highly irreversible and requires large overpotential [36]. Various nanomaterials have been immobilized on these electrodes to overcome this issue, resulting in a good elcctrocatalytic system [36,37]. In this study, we combined the huge specific surface area of CNTs and the excellent conductivity of IL to facilitate electrical communication between NADH and the modified electrode surface. As shown in Fig. 4A, CNTs-IL nanocomposites modified GCE showed an augmentation on the voltammetric and amperometric behaviors of electrocatalytic activity toward NADH. The addition of NADH resulted in a significant increase in the anodic current with a single oxidation peak at 0.06 V which is negative than lots of the carbon materials [36,37]. In conjunction with the good biocompatible of CNTs-IL [25], GDH was immobilized on the CNTs-IL nanocomposites electrode to construct a glucose biosensor.

Owing to the excellent film-forming ability, CS was used to entrap GDH on the CNTs-IL/GCD surface to fabricate nanocomposites-based biosensor. Fig. 4B showed CVs of the GDH-CS/CNT-IL/GCE with glucose concentrations from 0.02 mM to 1 mM. The oxidation peak current increased linearly within the glucose concentration up to 1 mM (as inset in Fig. 4B) with a detection limit of 9 μM (S/N = 3) and sensitivity of 5.3 μA mM^{-1}. According to the Lineweaver–Burk plot, Michaelis–Menten constant (K_m) of GDH entrapped by CS on CNTs-IL/GCE toward glucose was estimated to be 1.767 mM and smaller than reported ones of immobilized GDH [38], indicating that the CS is an excellent immobilizing matrix and the GDH entrapped by CS on CNTs-IL/GCE had high affinity to glucose.

The reproducibility of the resulting biosensor was investigated by five independently prepared electrodes with R.S.D. of 3.89% for 0.2 mM of glucose, suggesting a good reproducibility. The stability of the biosensor was evaluated by amperometric measurement after stored in 4 °C for 20 days and the current retained about 89% of its initial value, demonstrating the acceptable durability of the biosensor.

The biosensor was further applied to detect glucose in human serum for real application. Only a dilution of the serum with PBS was needed before detection. As shown in Table 1, three parallel measurement results were very close and the average concentration was 4.80 mM. The good recovery values range from 98.8% to 103.3% indicated good accuracy of the GDH-CS/CNTs-IL/GCE. These demonstrated that the proposed CNTs-IL nanocomposites-based biosensor was reliable and effective.

Table 1
Determination of glucose concentration in serum which was diluted to 20 times with PBS.

Number	Found in solution (mM)	Glucose in blood (mM)	Recovery (%)
1	0.244	4.88	101.8
2	0.243	4.86	103.3
3	0.233	4.66	98.8

4. Conclusion

In summary, a high-performance electrocatalytic platform based on CNTs integrated with environmentally friendly IL was constructed through π–π interaction between π electronic of CNT and the loop of imidazole IL. The hybrid nanocomposites showed a stable redox system with high electron transfer rate and performed good electrocatalytic activity toward O_2 and NADH at lower overpotential. Therefore an O_2 sensor and a glucose biosensor based on GDH were developed. The as prepared CNTs-IL nanocomposites electrodes showed good analytical performance and were applied to detect O_2 and glucose in real blood samples. These demonstrations pave an avenue for multiple functional electrochemical sensors.

Acknowledgments

This work was supported by the National Natural Science Foundation of China (21075116, 20935003, 20820102037) and 973 Project (2011CB911002, 2010CB933603).

References

[1] K.P. Gong, F. Du, Z.H. Xia, M. Durstock, L.M. Dai, Science 323 (2009) 760–764.
[2] L. Bai, Z. Zhou, Carbon 45 (2007) 2105–2110.
[3] S.J. Guo, S.J. Dong, E.K. Wang, Adv. Mater. 22 (2010) 1269–1272.
[4] B.S. Harrison, A. Atala, Biomaterials 28 (2007) 344–353.
[5] W.R. Yang, P. Thordarson, J.J. Gooding, S.P. Ringer, F. Braet, Nanotechnology 18 (2007) 1.
[6] G.L. Fu, X.L. Yue, Z.F. Dai, Biosens. Bioelectron. 26 (2011) 3973–3976.
[7] J. Wang, R.P. Deo, P. Poulin, M. Mangey, J. Am. Chem. Soc. 125 (2003) 14706–14707.
[8] C.B. Jacobs, M.J. Peairs, B.J. Venton, Anal. Chim. Acta 662 (2010) 105–127.

[9] H. Beitollahi, H. Karimi-Maleh, H. Khabazzadeh, Anal. Chem. 80 (2008) 9848–9851.
[10] S.Y. Deng, G.Q. Jian, J.P. Lei, Z. Hu, H.X. Ju, Biosens. Bioelectron. 25 (2009) 373–377.
[11] J.P. Kim, B.Y. Lee, J. Lee, S. Hong, S.J. Sim, Biosens. Bioelectron. 24 (2009) 3372–3378.
[12] S.K. Vashist, D. Zheng, K. Al-Rubeaan, J.H.T. Luong, F.-S. Sheu, Biotechnol. Adv. 29 (2011) 169–188.
[13] B.E.K. Swamy, B.J. Venton, Analyst 132 (2007) 876.
[14] J. Liu, A.G. Rinzler, H.J. Dai, J.H. Hafner, R.K. Bradley, P.J. Boul, A. Lu, T. Iverson, K. Shelimov, C.B. Huffman, F. Rodriguez-Macias, Y.S. Shon, T.R. Lee, D.T. Colbert, R.E. Smalley, Science 280 (1998) 1253–1256.
[15] X.H. Peng, S.S. Wong, Adv. Mater. 21 (2009) 625–642.
[16] T. Fukushima, T. Aida, Chem. Eur J. 13 (2007) 5048–5058.
[17] S.J. Guo, D. Wen, Y.M. Zhai, S.J. Dong, E.K Wang, Biosens. Bioelectron. 26 (2011) 3475–3481.
[18] L.P. Zhao, Y.J. Li, Z.F. Liu, H. Shimizu, Chem. Mater. 22 (2010) 5949–5956.
[19] T. Fukushima, A. Kosaka, Y. Ishimura, T. Yamamoto, T. Takigawa, N. Ishii, T. Aida, Science 300 (2003) 2072–2074.
[20] Y. Liu, S.J. Dong, Electrochem. Commun. 9 (2007) 1423–1427.
[21] L.H Lu, W. Chen, Adv. Mater. 22 (2010) 3745–3748.
[22] W. Lu, R. Hartman, L.T. Qu, L.M. Dai, J. Phys. Chem. Lett. 2 (2011) 655–660.
[23] Q. Wang, H. Tang, Q.J. Xie, L. Tan, Y.Y. Zhang, B.M. Li, S.Z. Yao, Electrochim. Acta 52 (2007) 6630–6637.
[24] Y. Liu, L. Liu, S.J. Dong, Electroanalysis 19 (2007) 55–59.
[25] Y. Liu, L.J. Huang, S.J. Dong, Biosens. Bioelectron. 23 (2007) 35–41.
[26] R. Marcilla, M.L. Curri, P.D. Cozzoli, M.T. Martínez, I. Loinaz, H. Grande, J.A. Pomposo, D. Mecerreyes, Small 2 (2006) 507–512.
[27] X.M. Wu, Y.J. Hu, J. Jin, N.L. Zhou, P. Wu, H. Zhang, C.X. Cai, Anal. Chem. 82 (2010) 3588–3596.
[28] A. Salimi, S. Lasghari, A. Noorbakhash, Electroanalysis 22 (2010) 1707–1716.
[29] L. Deng, Y.Z. Wang, L. Shang, D. Wen, F.A. Wang, S.J. Dong, Biosens. Bioelectron. 24 (2008) 951–957.
[30] M.K. Wang, Y. Shen, Y. Liu, T. Wang, F. Zhao, B.F. Liu, S.J. Dong, J. Electroanal. Chem. 578 (2005) 121–127.
[31] Z.A. Xu, N. Gao, H.J. Chen, S.J. Dong, Langmuir 21 (2005) 10808–10813.
[32] C.P. Andrieux, J.M. Dumasbouchiat, J.M. Saveant, J. Electroanal. Chem. 131 (1982) 1–35.
[33] S.Y. Wang, D.S. Yu, L.M. Dai, J. Am. Chem. Soc. 133 (2011) 5182–5185.
[34] P. Yu, J. Yan, H. Zhao, L. Su, J. Zhang, L.Q. Mao, J. Phys. Chem. C 112 (2008) 2177–2182.
[35] Y.M. Yan, W. Zheng, L. Su, L.Q. Mao, Adv. Mater. 18 (2006) 2639–2643.
[36] M. Zhou, L. Shang, B.L. Li, L.J. Huang, S.J. Dong, Biosens. Bioelectron. 24 (2008) 442–447.
[37] M. Zhou, Y.M. Zhai, S.J. Dong, Anal. Chem. 81 (2009) 5603–5613.
[38] J. Razumiene, R. Meškys, V. Gureviciene, V. Laurinavicius, M.D. Reshetova, A.D. Ryabov, Electrochem. Commun. 2 (2000) 307–311.